

# A Quadratic Programming Framework for Constrained and Robust Jet Engine Health Monitoring

*S. Borguet and O. Léonard  
University of Liège, Turbomachinery Group  
Chemin des Chevreuils 1, B-4000 Liège, Belgium  
{s.borguet,o.leonard}@ulg.ac.be*

## Abstract

Kalman filters are largely used in the jet engine community for condition monitoring purpose. This algorithm gives a good estimate of the engine condition provided that the residuals between the model prediction and the measurements are zero-mean, Gaussian random variables. In the case of sensor faults, this assumption does not hold anymore and consequently the diagnosis is spoiled.

This contribution presents a recursive estimation algorithm based on a Quadratic Programming formulation which provides robustness against sensor faults and allows constraints on the health parameters to be specified. The improvements in estimation accuracy brought by this new algorithm are illustrated by a series of typical test-cases that may be encountered on current turbofan engines.

## Nomenclature

$(\hat{\cdot})$	estimated value
$(\cdot)^-$	prior value
A8IMP	nozzle exit area (nominal value: 1.4147 m <sup>2</sup> )
<b>b</b>	the sensor fault vector
hpc	high pressure compressor
hpt	high pressure turbine
$k$	discrete time index
KF	Kalman Filter
lpc	low pressure compressor
lpt	low pressure turbine
$p_i^0$	total pressure at station $i$
QP	Quadratic Programming
SEi	efficiency factor at station $i$ (nominal value: 1.0)
SFDI	Sensor Fault Detection and Isolation
SWiR	flow capacity factor at station $i$ (nominal value: 1.0)
$T_i^0$	total temperature at station $i$
<b>u</b>	operating point parameters
<b>w</b>	health parameters
<b>y</b>	observed measurements
$\epsilon$	measurement noise vector
$\omega$	process noise vector
$\sigma$	nominal standard deviation of the sensors
$\mathcal{N}(\mathbf{m}, \mathbf{R})$	a Gaussian probability distribution with mean <b>m</b> and covariance matrix <b>R</b>

## Introduction

Over the last decades, significant research efforts have been undertaken to develop efficient condition monitoring tools for jet engines. The information about the engine health allows a condition-based maintenance to be set up which leads to improved safety and operability as well as reduced life cycle costs.

In this paper, Module Performance Analysis, aka. Gas Path Analysis, is considered. Its purpose is to assess the changes in engine module performance, described by so-called health parameters, on the basis of measurements collected along the gas path of the engine [1]. Typically, the health parameters are correcting factors on the efficiency and flow capacity of the components (fan, lpc, hpc, hpt, lpt, nozzle) while the measurements are component temperatures, pressures and shaft speeds. Among the many available techniques to solve this problem, the Kalman filter is one of the most popular.

The engine deteriorates during its exploitation. Besides component faults, sensor (instrumentation) faults may occur too. Loosely speaking, a sensor fault is a data generated by a device whose behaviour does no longer follow the manufacturer characteristics. Instrumentation faults can be classified as systematic errors, such as biases and drifts, or as impulsive noise which are random “spikes” in the measured data. These instrumentation faults can spoil the estimation of the engine condition. It is therefore mandatory to make diagnosis tools robust against sensor faults. A variety of solutions have been studied in the community such as *data filtering* [2, 3], *instrumental variables* [4, 5, 6], *banks of Kalman filters* [7, 8] or *robust estimation techniques* [9, 10, 11].

One of the drawbacks associated to robust estimation is that the estimation problem becomes non-linear even in the case of a linear system model. The consequence is an increase in the computational load. However, it has been shown that the robust estimation problem can be transformed into a *Quadratic Programming* (QP) problem [12] for which efficient solvers are available. The authors have reported in a previous publication the development of a robust algorithm for performance monitoring using this QP formulation [13].

Sometimes, additional information about the health parameters is available, such as constraints based on physical considerations (e.g. aerodynamic efficiencies are not expected to improve over time). Yet, they are generally disregarded in the estimation process because they do not fit into the structure of the Kalman filter. Some research [14, 15] has been dedicated to this issue and has shown improved accuracy on the estimated quantities at the price of a tedious inclusion of the constraints. The Quadratic Programming approach allows the integration of those constraints in an easy way.

In the light of these considerations, the present contribution reports the formulation of a recursive Quadratic Programming algorithm for robust and constrained engine performance monitoring. The novelty lies in the natural inclusion of constraints on the health parameters in the estimation problem and in a wise, recursive implementation. The benefit in terms of stability and accuracy brought by this new methodology is illustrated for several sensor faults that may be encountered on a jet engine.

## Statement of the Problem

The scope of this section is to underline the sensitivity of the Kalman filter with respect to outliers, then to present the approach to turn the robust estimation problem into a QP one. Finally, the inclusion of constraints on the health parameters and the structure of the resulting algorithm are discussed.

### Kalman Filter Basics

A number of researchers have used the celebrated Kalman filter [16] in order to assess the health parameters. One of the master pieces of this algorithm is a simulation model of the monitored process. In the framework of gas path analysis, these are generally non-linear aero-thermodynamic models based on mass, energy and momentum conservation laws applied to the engine flowpath. Equation (1) represents such an engine model where  $k$  is a discrete time index,  $\mathbf{u}_k$  are the parameters defining the operating point of the engine (e.g. fuel flow, altitude, Mach number),  $\mathbf{w}_k$  are the aforementioned health parameters and  $\mathbf{y}_k$  are the gas path measurements. A random variable  $\epsilon_k \in \mathcal{N}(\mathbf{0}, \mathbf{R}_y)$  which accounts for sensor inaccuracies is added to the deterministic part  $\mathcal{G}(\cdot)$  of the model.

$$\mathbf{y}_k = \mathcal{G}(\mathbf{u}_k, \mathbf{w}_k) + \epsilon_k \quad (1)$$

A common interpretation of the Kalman filter is that of a recursive, maximum a posteriori approach to parameter

identification. Both the health parameters and the measurements are considered as Gaussian random variables<sup>1</sup>. Within this framework, the estimated health parameters are obtained by minimising the following objective function:

$$\mathcal{J}(\mathbf{w}_k) = \frac{1}{2}(\mathbf{w}_k - \widehat{\mathbf{w}}_k^-)^T (\mathbf{P}_{\mathbf{w},k}^-)^{-1} (\mathbf{w}_k - \widehat{\mathbf{w}}_k^-) + \frac{1}{2} \mathbf{r}_k^T \mathbf{R}_r^{-1} \mathbf{r}_k \quad (2)$$

The first term in the right hand side of equation (2) forces the identified parameters to lie in a neighbourhood of prior values  $\widehat{\mathbf{w}}_k^-$ . The prior covariance matrix  $\mathbf{P}_{\mathbf{w},k}^-$  specifies the shape of this region and summarises the information contained in the measurement history up to time  $k-1$ . The second term expresses a weighted-least-squares criterion. Considering an update mechanism based on a semi-linear Kalman filter, the residuals  $\mathbf{r}_k$  are approximated with:

$$\begin{aligned} \mathbf{r}_k &= \mathbf{y}_k - \widehat{\mathbf{y}}_k \\ &= \mathbf{y}_k - \left[ \widehat{\mathbf{y}}_k + \mathbf{G} (\mathbf{w}_k - \widehat{\mathbf{w}}_k^-) \right] \\ &= \widehat{\mathbf{r}}_k - \mathbf{G} (\mathbf{w}_k - \widehat{\mathbf{w}}_k^-) \end{aligned} \quad (3)$$

where

$$\begin{aligned} \widehat{\mathbf{y}}_k &= \mathcal{G}(\mathbf{u}_k, \widehat{\mathbf{w}}_k^-) \\ \mathbf{G} &= \left. \frac{\partial}{\partial \mathbf{w}_k} \mathcal{G}(\mathbf{u}_k, \mathbf{w}_k) \right|_{\mathbf{w}_k = \mathbf{w}^{hl}} \end{aligned} \quad (4)$$

are respectively the a priori prediction of the measurements and the Jacobian matrix of the engine model around nominal values  $\mathbf{w}^{hl}$  of the health parameters. The residuals are weighted with a covariance matrix  $\mathbf{R}_r$  that takes into account the fact that both the measurements and the operating conditions are sensed – and hence noisy – before being fed in the Kalman filter:

$$\mathbf{R}_r = \mathbf{R}_y + \mathbf{H}^T \mathbf{R}_u \mathbf{H} \quad (5)$$

where

$$\mathbf{H} = \frac{\partial}{\partial \mathbf{u}_k} \mathcal{G}(\mathbf{u}_k, \mathbf{w}_k)$$

is the influence matrix between the operating conditions and the measurements and  $\mathbf{R}_u$  is the covariance matrix of the noise on the measured operating conditions.

To generate the a priori values of the health parameter distribution (i.e. mean  $\widehat{\mathbf{w}}_k^-$  and covariance  $\mathbf{P}_{\mathbf{w},k}^-$ ), a model describing the temporal evolution of the parameters must be supplied as well. Generally, few information is available about the way the engine degrades which motivates the choice of a random walk model:

$$\mathbf{w}_k = \mathbf{w}_{k-1} + \omega_k \quad (6)$$

where  $\omega_k \in \mathcal{N}(\mathbf{0}, \mathbf{Q}_k)$  is the so-called process noise that provides some adaptability to track a time-evolving fault.

Algorithm 1 summarises in a pseudo-code style the architecture of the Kalman filter. This algorithm has a predictor-corrector structure. On line 2, prediction of the prior values of the health parameter distribution are made thanks to the transition model (6). Then the data are acquired and used for building the a priori residuals (lines 3 and 4). The Kalman gain  $\mathbf{K}$  is then computed on line 5. Loosely speaking, it weights the uncertainty on the parameters versus the one on the measurements. Finally, the a posteriori distribution is assessed at the corrector step (line 6). This update rule for the health parameters is obtained by cancelling out the first order derivatives of equation (2):

$$(\mathbf{P}_{\mathbf{w},k}^-)^{-1} (\mathbf{w}_k - \widehat{\mathbf{w}}_k^-) - \mathbf{G}_k^T \mathbf{R}_y^{-1} \mathbf{r}_k = 0 \quad (7)$$

The interested reader may consult reference [17] for an extensive derivation and additional details.

<sup>1</sup>statistically, they are hence thoroughly defined by their mean and covariance matrix

**Algorithm 1** Semi-linear Kalman filter

---

**Require:**  $\widehat{\mathbf{w}}_0, \mathbf{P}_{\mathbf{w},0}, \mathbf{R}_r, \mathbf{Q}_k$

- 1: **for**  $k > 0$  **do**
- 2:    $\widehat{\mathbf{w}}_k^- = \mathbf{w}_{k-1}$  and  $\mathbf{P}_{\mathbf{w},k}^- = \mathbf{P}_{\mathbf{w},k-1} + \mathbf{Q}_k$
- 3:   acquire  $\mathbf{u}_k$  and  $\mathbf{y}_k$
- 4:    $\widehat{\mathbf{r}}_k = \mathbf{y}_k - \mathcal{G}(\mathbf{u}_k, \widehat{\mathbf{w}}_k^-)$
- 5:    $\mathbf{K} = \mathbf{P}_{\mathbf{w},k}^- \mathbf{G}^T (\mathbf{G} \mathbf{P}_{\mathbf{w},k}^- \mathbf{G}^T + \mathbf{R}_r)^{-1}$
- 6:    $\widehat{\mathbf{w}}_k = \widehat{\mathbf{w}}_k^- + \mathbf{K} \widehat{\mathbf{r}}_k$  and  $\mathbf{P}_{\mathbf{w},k} = (\mathbf{I} - \mathbf{K} \mathbf{G}) \mathbf{P}_{\mathbf{w},k}^-$
- 7: **end for**

---

**From Kalman Filtering to Robust QP Estimation**

One of the assumptions in the derivation of the Kalman filter is the zero-mean, Gaussian nature of the measurement noise. The quadratic penalisation of the residuals in the objective function (2) derives directly from this hypothesis and makes the algorithm very sensitive to large residuals. Consequently, even a small amount of outliers can strongly deteriorate the quality of the estimation.

Robust estimation techniques aim at lowering the sensitivity with respect to large residuals by replacing the Gaussian probability density function by another noise distribution prone to outliers. Among the many candidate distributions, the so-called  $\delta$ -contaminated function (aka. Huber's function) has received much attention in the literature and is selected in this contribution. A detailed description of this function is beyond the scope of this paper, but can be found in reference [19]. Basically, Huber's function consists in a Gaussian random variable contaminated by a fraction  $\delta$  of outliers.

Mathematically, the linear dependency in the residuals  $\mathbf{r}_k$  in equation (7) is replaced with a function  $\psi(\mathbf{r}_k)$  that lowers the influence of large residuals:

$$(\mathbf{P}_{\mathbf{w},k}^-)^{-1}(\mathbf{w}_k - \widehat{\mathbf{w}}_k^-) - \mathbf{G}_k^T \mathbf{R}_y^{-1} \psi(\mathbf{r}_k) = 0 \quad (8)$$

Huber's weighting function is sketched in figure 1 for a scalar random variable  $\epsilon$ . Mathematically, it can be written as:

$$\psi(\epsilon) = \max(-\Delta\sigma, \min(\epsilon, \Delta\sigma)) \quad (9)$$

where  $\sigma$  is the standard deviation of the “clean” Gaussian variable and the scalar  $\Delta$  is a threshold depending on the contamination level  $\delta$  (e.g.  $\Delta=1.399$  for  $\delta=0.05$ ).

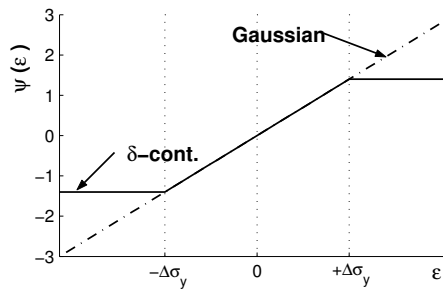


Figure 1: Huber's weighting function for a scalar

Adopting Huber's function as the penalisation function of the residuals increases the robustness against sensor faults, but turns the simple linear function (7) for parameter update into a non-linear one. No explicit update formula can be obtained and relation (8) must be solved numerically, with Newton's method for instance. This might be cumbersome for on-line applications.

Nonetheless, it is shown in [12] that the non-linear program resulting from the choice of a noise distribution following Huber's law can be transformed into a quadratic program for which efficient and fast solvers are available [20]. In

[13], the authors have derived a Sensor Fault Detection and Isolation module based on this formulation which has been integrated with a tool for engine performance monitoring. As a reminder, the milestones are reported below.

As a first step, a vector  $\mathbf{b}_k$  is introduced in the measurement equation (1) to model the outliers:

$$\mathbf{y}_k = \mathcal{G}(\mathbf{u}_k, \mathbf{v}_k, \mathbf{w}_k, \mathbf{x}_k) + \mathbf{b}_k + \boldsymbol{\epsilon}_k \quad (10)$$

The objective function of the robust estimation problem becomes<sup>2</sup>:

$$\begin{aligned} \mathcal{J}(\mathbf{w}_k, \mathbf{b}_k) = & \frac{1}{2}(\mathbf{w}_k - \widehat{\mathbf{w}}_k^-)^T (\mathbf{P}_{\mathbf{w},k}^-)^{-1} (\mathbf{w}_k - \widehat{\mathbf{w}}_k^-) \\ & + \frac{1}{2} \mathbf{r}_k^T \mathbf{R}_y^{-1} \mathbf{r}_k + \Delta \boldsymbol{\sigma}^{-T} |\mathbf{b}_k| \end{aligned} \quad (11)$$

The equivalence between solving equation (8) for  $\mathbf{w}_k$  with Huber's  $\psi$  function and minimising the objective function (11) with respect to  $\mathbf{w}_k$  and  $\mathbf{b}_k$  is established in [12]. It should be pointed out that the criterion (11) is convex and therefore admits a unique optimum.

Finally, the quantities  $\mathbf{b}_k$  and  $|\mathbf{b}_k|$  are replaced with their positive and negative parts in order to transform the objective function (11) into a quadratic one:

$$\begin{cases} \mathbf{b}_k = \mathbf{b}_k^+ - \mathbf{b}_k^- \\ |\mathbf{b}_k| = \mathbf{b}_k^+ + \mathbf{b}_k^- \end{cases} \quad \text{with} \quad \begin{cases} \mathbf{b}_k^+ = \max(\mathbf{b}_k, 0) \\ \mathbf{b}_k^- = -\min(\mathbf{b}_k, 0) \end{cases} \quad (12)$$

With this change of variables, the objective function writes down:

$$\begin{aligned} \mathcal{J}(\mathbf{w}_k, \mathbf{b}_k^+, \mathbf{b}_k^-) = & \frac{1}{2}(\mathbf{w}_k - \widehat{\mathbf{w}}_k^-)^T (\mathbf{P}_{\mathbf{w},k}^-)^{-1} (\mathbf{w}_k - \widehat{\mathbf{w}}_k^-) \\ & + \frac{1}{2} \mathbf{r}_k^T \mathbf{R}_y^{-1} \mathbf{r}_k + \Delta \boldsymbol{\sigma}^{-T} (\mathbf{b}_k^+ + \mathbf{b}_k^-) \end{aligned} \quad (13)$$

### Constraints Handling in the KF and QP Frameworks

In the case of condition monitoring, additional information about the health parameters is generally available. For instance, assuming that no maintenance actions are undertaken, the aerodynamic efficiencies of compressors and turbines are expected not to improve over time. These constraints actually increase in some way the a priori knowledge and should therefore be taken into account in the estimation problem.

Unfortunately, the Kalman filter algorithm does not allow such constraints to be easily integrated. Two solutions have been investigated in the literature. On the one hand, the soft-constrained approach (see[15]) modifies the objective function (2) by adding a third term analogous to the first one and which forces the posterior values of the health parameters to stand in some neighbourhood of the constrained values. While quite easy to understand, this technique ensures the respect of the constraints only on average. Moreover, from a user's standpoint, it may turn quite difficult to tune the various involved parameters (such as shape and size of the neighbourhood).

On the other hand, the hard-constrained approach aims at enforcing the constraints at each time step. In [14], a two-step procedure is proposed. First, a regular Kalman filter estimates the parameters, which are seen as an unconstrained solution. Then, a QP problem is solved that projects the unconstrained solution inside the constraint boundary. The constrained solution possesses a number of interesting properties that are proved in [14]. This solution looks quite appealing, but makes the algorithm more complex due to the addition of the projection problem.

The QP formulation introduced in the previous section for robust estimation offers the required framework to include seamlessly constraints on the health parameters. Note that the variables  $\mathbf{b}_k^+$  and  $\mathbf{b}_k^-$  are already forced to be non-negative through their very definition, cf. equation (12). Similarly, side constraints – or even linear inequality constraints – can be set on the health parameters. In the present application, only side constraints are considered. Bounds can be specified either for the parameter itself, or for its derivative as shown in equations (14-15) for the case of upper bounds.

<sup>2</sup>note that the residuals  $\mathbf{r}_k$  are a linear function of  $\mathbf{w}_k$  and  $\mathbf{b}_k$  through equations (3) and (10)

$$\mathbf{w}_k(j) \leq \mathbf{w}^{up}(j) \quad (14)$$

$$\mathbf{w}_k(j) \leq \widehat{\mathbf{w}}_{k-1}(j) + \delta \mathbf{w}^{up}(j) = \mathbf{w}_k^{up}(j) \quad (15)$$

where  $j$  is the index of the constrained health parameter,  $\mathbf{w}^{up}$  and  $\delta \mathbf{w}^{up}$  are the upper bounds respectively on the parameters and on their increment per time step.

Considering the performance tracking of a turbofan engine, it is known that the efficiency of all components and the flow capacities of the compressors decrease with usage. Accordingly, constraints of type (15) are set on the corresponding health parameters. Ideally, the bounds  $\delta \mathbf{w}^{up}$  on the rate of variation should be set to zero to reflect the deterioration. Nonetheless, they are set in practice to a small positive value because the estimates may oscillate around the true value.

### Practical Implementation of the Algorithm

As a result of the inclusion of robustness and constraints in the estimation problem, the updated parameters are obtained by solving the following quasi-unconstrained Quadratic Problem:

$$\min_{\mathbf{w}_k, \mathbf{b}_k^+, \mathbf{b}_k^-} \mathcal{J}(\mathbf{w}_k, \mathbf{b}_k^+, \mathbf{b}_k^-) \quad \text{subject to} \quad \begin{cases} \mathbf{b}_k^+ \geq 0 \\ \mathbf{b}_k^- \geq 0 \\ \mathbf{w}_k(j) \leq \mathbf{w}_k^{up}(j), j \in \text{the set of constrained parameters} \end{cases} \quad (16)$$

The Kalman filter structure serves as a basis in order to derive a recursive algorithm based on the QP formulation. It can be seen in algorithm 1 that the Kalman filter propagates the mean and the covariance matrix of the health parameter distribution. Yet, it can also be noted that in the objective function (13), the inverse of the covariance matrix appears. Therefore, the developed recursive QP algorithm rather updates this inverted covariance matrix, aka. the information matrix,  $\Gamma_{\mathbf{w},k} = \mathbf{P}_{\mathbf{w},k}^{-1}$  (see [18] for further details). The pseudo-code of the resulting algorithm is proposed in algorithm 2. It can be noticed that the computation of the a priori information matrix requires a matrix inversion (line 2) while the update of the information matrix is a simple matrix addition (line 6). As previously mentioned, the explicit update rule for the health parameters is replaced with the numerical solution of (16).

---

#### Algorithm 2 Recursive QP estimation procedure

---

**Require:**  $\widehat{\mathbf{w}}_0, \Gamma_{\mathbf{w},0}, \mathbf{R}_r^{-1}, \mathbf{Q}_k^{-1}$ , set of constraints

- 1: **for**  $k > 0$  **do**
  - 2:    $\widehat{\mathbf{w}}_k^- = \mathbf{w}_{k-1}$  and  $\Gamma_{\mathbf{w},k}^- = \Gamma_{\mathbf{w},k-1} - \Gamma_{\mathbf{w},k-1} (\Gamma_{\mathbf{w},k-1} + \mathbf{Q}_k^{-1})^{-1} \Gamma_{\mathbf{w},k-1}$
  - 3:   acquire  $\mathbf{u}_k$  and  $\mathbf{y}_k$
  - 4:    $\widehat{\mathbf{r}}_k^- = \mathbf{y}_k - \mathcal{G}(\mathbf{u}_k, \widehat{\mathbf{w}}_k^-)$
  - 5:   solve QP problem (16) to obtain  $\widehat{\mathbf{w}}_k$
  - 6:    $\Gamma_{\mathbf{w},k} = \Gamma_{\mathbf{w},k}^- + \mathbf{G}^T \mathbf{R}_r^{-1} \mathbf{G}$
  - 7: **end for**
- 

## Application Example

### Engine Layout

The application considered as a test-case is a large bypass ratio, mixed-flow, turbofan. The engine performance model has been developed in the frame of the OBIDICOTE<sup>3</sup> project and is detailed in [22]. A schematic of the engine is sketched in figure 2 where the location of the eleven health parameters and the station numbering are also indicated. One command variable, namely the fuel flow rate fed in the combustor, is considered in the following.

The sensor suite selected for tracking the performance degradation is representative of the instrumentation available on-board contemporary turbofan engines and is detailed in table 1 where the accuracy of each sensor is reported too. The

---

<sup>3</sup>A Brite-Euram project for On-board Identification, Diagnosis and Control of Turbofan Engine

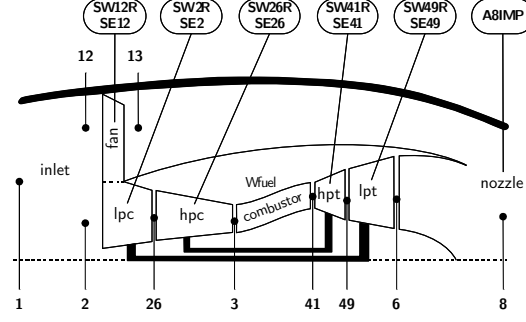


Figure 2: Turbofan layout with health parameters' location

upper four sensors define the operating conditions (fuel flow, inlet total pressure and temperature, ambient pressure) and the remaining eight are the gas path sensors. In this configuration, the number of health parameters to estimate exceeds the number of gas path sensors. Therefore, if a sensor fault occurs, it is likely that several combinations of the health parameter deviations exactly reproduce the sensor fault, thus leading to a wrong diagnosis of the engine condition. To allow the simultaneous detection of sensor and component faults, the redundancy must consequently be increased.

Table 1: Sensor configuration (uncertainty is three times the standard deviation)

Label	Uncertainty	Label	Uncertainty
$W_{fuel}$	$\pm 2$ g/s	$T_1^0$	$\pm 2$ K
$p_1^0$	$\pm 100$ Pa	$p_{amb}$	$\pm 100$ Pa
$p_{13}^0$	$\pm 100$ Pa	$T_{26}^0$	$\pm 2$ K
$p_{26}^0$	$\pm 500$ Pa	$T_3^0$	$\pm 2$ K
$p_3^0$	$\pm 5000$ Pa	$T_6^0$	$\pm 2$ K
$N_{lp}$	$\pm 6$ RPM	$N_{hp}$	$\pm 12$ RPM

In the present application, the redundancy is extended by taking into account the fact that, on modern engines, the instrumentation is generally “dual-channeled”: each of the eight probes is connected to two independent lanes (sensing element and signal processing hardware). As a result, 16 measurements are available which provides the necessary redundancy to perform the robust estimation problem. It must be pointed out that this trick does not modify the observability of the health parameters, which is linked to the variety in the sensor suite.

### Definition of the Test-Cases

A series of test-cases has been designed to assess the efficiency of the new robust and constrained estimation technique. Due to non-availability of real data, simulated ones are used instead. Cruise conditions (Alt = 10800m, Mach = 0.82,  $\Delta T_{ISA} = 0$  K) are assumed. The flight sequence is 5000 seconds long and the sampling rate is set to 2 Hz. Gaussian noise, whose magnitude is specified in table 1 is added to the generated measurements to make them closer to real ones.

The engine wear is simulated from the component fault case proposed in [23]. It consists in a drift of nearly all health parameters, starting from a healthy engine (all parameters at their nominal values) at  $t=0$  s and with the following degradation at the end of the sequence ( $t=5000$  s):  $-1.5\%$  on SW12R,  $-1.2\%$  on SE12,  $-1.0\%$  on SW2R,  $-1.0\%$  on SE2,  $-2.3\%$  on SW26R,  $-1.4\%$  on SE26,  $+0.88\%$  on SW41R,  $-1.6\%$  on SE41,  $-1.3\%$  on SE49.

Three types of sensor faults are investigated in the test-cases: impulsive noise (spikes), sensor bias and sensor drift. The sign of the sensor fault must also be accounted for, this results in six types of sensor faults which are summarised in table 2.

The level of impulsive noise per sensor is set to 5%, which means that on average, 5 out of 100 samples are aberrant. The magnitude is set to  $\pm 10$  times the standard deviation. For the biases, only one sensor is simulated faulty at a time.

Table 2: Description of the sensor faults

Case	Description	Magnitude
a	5 % impulsive noise	$+10 \sigma$
b	5 % impulsive noise	$-10 \sigma$
c	sensor bias	$+5 \sigma$
d	sensor bias	$-5 \sigma$
e	sensor drift	$+10 \sigma$
f	sensor drift	$-10 \sigma$

The bias starts at  $t=1000$  s and does not evolve till the end of the sequence. Considering the drifts, only one sensor is simulated faulty at a time as well. The drift starts at time  $t=1000$  s with a magnitude of zero and reaches a magnitude of  $\pm 10$  standard deviation at  $t=5000$  s. The magnitudes of the sensor faults have been selected according to contributions from members of the OBIDICOTE project.

### Figure of Merit

It is proposed to compare the efficiency of three estimation tools which are the standard *Kalman filter* (KF), the *robust QP* (QPR) and the *robust and constrained QP* (QPRC). To this end, a figure of merit consisting in the maximum Root Mean Squared Error (RMSE) over the whole sequence is defined:

$$e_{RMS} = \max \left( \sqrt{\frac{1}{n} \sum_{k=1}^n \left( \frac{\mathbf{w}_k - \widehat{\mathbf{w}}_k}{\mathbf{w}^{hl}} \right)^2} \right) \quad (17)$$

where  $\mathbf{w}^{hl}$  are the nominal values of the health parameters.

Given the stochastic nature of the measurement noise, each test-case has been run twenty times and the RMSEs reported in tables 3-5 are the average over those twenty runs in order to guarantee that they are statistically representative. A test-case characterised by an averaged maximum RMSE below 0.25% is declared as successful which is indicated by a checkmark. This threshold corresponds to three times the standard deviation of the identified health parameters (*i.e.* the square root of the diagonal terms of the covariance matrix  $\mathbf{P}_{\mathbf{w},k}$ ).

### Results – Impulsive Noise

In table 3, the figures of merit are reported for the test-cases involving no sensor fault and impulsive noise (fault types a and b). The three algorithms achieve roughly the same accuracy when none of the sensors is faulty. It can be seen that the standard Kalman filter is unable to correctly track the engine condition when spikes pollute the data. This underlines the high sensitivity of least-square-based methods with respect to outliers. On the contrary, the robust QP algorithm, constrained or not, is not perturbed by the impulsive noise. For the present case, the inclusion of constraints on the health parameters does not improve the estimation.

Table 3: Comparison of the figure of merit  $e_{RMS}$  in the case of no sensor fault (nosf) and impulsive noise

Fault case	KF	QPR	QPRC
nosf	0.08 % ✓	0.10 % ✓	0.09 % ✓
a	0.78 % -	0.10 % ✓	0.10 % ✓
b	0.59 % -	0.09 % ✓	0.10 % ✓



## Results – Sensor Biases

The figures of merit of the three algorithms in the case of a biased sensor are given in table 4. It can be noticed that the Kalman filter is unable to perform an accurate diagnosis of the engine condition when only one of the sixteen sensors is biased. This is a further illustration of the sensitivity of the Kalman filter to aberrant data. Considering both robust tools, they seem unaffected by the biased sensor and have nearly the same efficiency as for the no-fault case. The proposed robust estimation approach allows indeed the detection and isolation of the faulty sensor which results in an accurate assessment of the engine health.

Here again, the constrained and robust QP algorithm (QPRC) does not perform better than the unconstrained one (QPR). This can be explained by the fact that the robust criterion has a classification nature (see Huber's function (9) and figure 1) and therefore it isolates sensor biases quite naturally. The sensor fault being correctly identified, its contribution is removed from the estimation process. As a result, adding constraints on the health parameters does not provide any supplemental advantage.

Table 4: Comparison of the figure of merit  $e_{RMS}$  in the case of sensor biases

Faulty Sensor	case c: $+5\sigma$ bias			case d: $-5\sigma$ bias		
	KF	QPR	QPRC	KF	QPR	QPRC
$p_{13}^0$	0.71 % -	0.10 % ✓	0.08 % ✓	0.68 % -	0.10 % ✓	0.11 % ✓
$p_{26}^0$	0.82 % -	0.09 % ✓	0.08 % ✓	0.62 % -	0.11 % ✓	0.11 % ✓
$T_{26}^0$	1.91 % -	0.14 % ✓	0.12 % ✓	1.84 % -	0.10 % ✓	0.09 % ✓
$p_3^0$	0.76 % -	0.10 % ✓	0.08 % ✓	0.63 % -	0.10 % ✓	0.07 % ✓
$T_3^0$	0.69 % -	0.10 % ✓	0.08 % ✓	0.69 % -	0.10 % ✓	0.08 % ✓
$N_{lp}$	0.76 % -	0.09 % ✓	0.09 % ✓	0.62 % -	0.10 % ✓	0.08 % ✓
$N_{hp}$	0.76 % -	0.10 % ✓	0.08 % ✓	0.61 % -	0.12 % ✓	0.08 % ✓
$T_6^0$	0.86 % -	0.10 % ✓	0.08 % ✓	0.55 % -	0.12 % ✓	0.08 % ✓

## Results – Sensor Drifts

The performance of the diagnosis tools when the data is contaminated by a drifting reading on one sensor is presented in table 5. As for the sensor bias cases, the regular Kalman filter is totally fooled by the drifting sensor and the resulting health assessment is spoiled. It can also be seen that the QPR algorithm provides an accurate estimation in all but three cases which are a positive drift on fan bypass outlet pressure  $p_{13}^0$ , and a negative drift on high pressure spool speed  $N_{LP}$  and on exhaust gas temperature  $T_6^0$ . For those three cases, the QPR algorithm erroneously assigns the sensor fault to the healthy lane. As a result, the health parameters are adapted so as to cope with the real engine condition and with the faulty sensor channel. This misclassification of the sensor fault is due to its nature. Indeed, the drift starts with a null magnitude and increases linearly with a soft slope. Hence, in the early moments after it appears, the drift has a magnitude lower than the threshold of the robust criterion. Moreover, classical Gaussian noise is superimposed to this drift which makes the detection task even more difficult.

Table 5: Comparison of the figure of merit  $e_{RMS}$  in the case of sensor drifts

Faulty Sensor	case e: $+10\sigma$ drift			case f: $-10\sigma$ drift		
	KF	QPR	QPRC	KF	QPR	QPRC
$p_{13}^0$	1.27 % -	<b>1.18 %</b> -	0.09 % ✓	0.70 % -	0.10 % ✓	0.10 % ✓
$p_{26}^0$	0.98 % -	0.10 % ✓	0.08 % ✓	1.09 % -	0.20 % ✓	0.14 % ✓
$T_{26}^0$	3.59 % -	0.21 % ✓	0.14 % ✓	3.47 % -	0.14 % ✓	0.10 % ✓
$p_3^0$	0.84 % -	0.10 % ✓	0.08 % ✓	1.00 % -	0.09 % ✓	0.07 % ✓
$T_3^0$	0.80 % -	0.10 % ✓	0.08 % ✓	0.92 % -	0.09 % ✓	0.08 % ✓
$N_{lp}$	0.82 % -	0.10 % ✓	0.08 % ✓	0.94 % -	0.10 % ✓	0.10 % ✓
$N_{hp}$	0.80 % -	0.10 % ✓	0.07 % ✓	1.56 % -	<b>0.94 %</b> -	0.14 % ✓
$T_6^0$	1.14 % -	0.10 % ✓	0.07 % ✓	1.16 % -	<b>0.68 %</b> -	0.10 % ✓

Correct isolation of every sensor drift might be achieved by enhancing the variety in the sensor suite. Another solution is to increase the available information by specifying constraints on the health parameters as has been discussed in a previous section. The figures of merit related to the QPRC algorithm in effect show that it is a wise solution which allows all test-cases to be accurately solved.

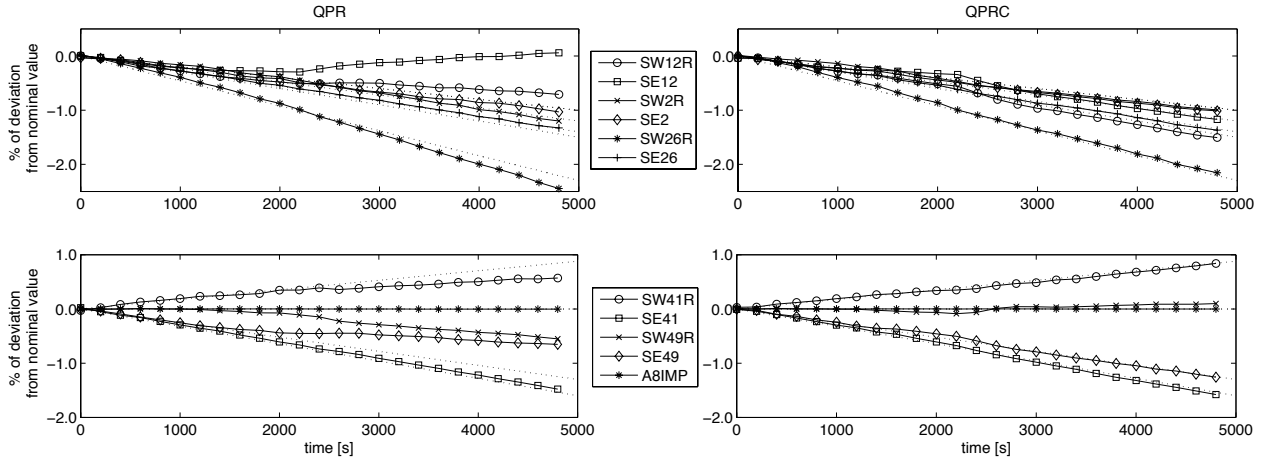


Figure 3: Identification of the health parameters by the QPR (left) and QPRC (right) algorithms with a positive drift on  $p_{13}^0$  – dotted lines show actual parameter values

To conclude this short analysis of the results, figure 3 sketches the evolution of the identified health parameters in the case of a drift on  $p_{13}^0$ . The left column is related to the QPR algorithm while the right column is related to the QPRC algorithm. The upper graphs show the parameters of the compressors and the lower ones, the parameters of the turbines and nozzle. Looking at the QPR results, it can be noticed that the misclassification of the drifting sensor leads to an error in the estimation of all parameters and particularly SE12, SW41R, SW49R and SE49. It is also interesting to point out that the fan efficiency factor SE12 improves from about 2000 s which is not a physical solution.

The addition of constraints on the rate of variation on all efficiency factors and on the compressor flow factors solves this issue as can be seen from the QPRC results. Around 2000 s seconds, the slope of SE12 and SE49 decreases as in the unconstrained case. However, the constraints limit this effect which eases the identification of the true faulty sensor. Then, the estimated health parameters track their actual values. A similar analysis can be conducted for the case of a drift on  $N_{LP}$  and on  $T_6^0$ .

## Conclusions

In this contribution, an original algorithm for constrained and robust estimation of engine condition has been proposed based on a Quadratic Programming approach. The proposed methodology can be considered as a generalisation of the Kalman filter which brings robustness against sensor faults and allows constraints to be set easily on the estimated parameters. The improvement in estimation efficiency have been illustrated on a number of virtual, but still realistic test-cases. The robust estimation tool can cope accurately with impulsive noise and sensor biases. By adding constraints which are physically meaningful, the robust and constrained estimation tool is made insensitive to sensor drifts.

Those results are promising, yet a number of issues have to be addressed in future research. The first question of practical interest is to determine the minimum level of bias for each sensor that can be effectively isolated by the robust algorithm. A second point is to make the present algorithm, which is primarily dedicated to performance monitoring, capable to track abrupt variation of the engine condition. This is a challenging problem as an abrupt component fault could be interpreted as a combination of sensor biases.

## References

- [1] A. J. Volponi, *Foundation of Gas Path Analysis (part i and ii)*, von Karman Institute LS03-01 : Gas Turbine Condition Monitoring and Fault Diagnosis, 2003.
- [2] H. Liu, S. Shah, W. Jiang, *On-line Outlier Detection and Data Cleaning*, Computers and Chemical Engineering, vol. 28, 2004.
- [3] V. Surrender, R. Ganguli, *Adaptive Myriad Filter for Improved Gas Turbine Condition Monitoring using Transient Data*, ASME Paper GT2004-53080, 2004.
- [4] A.J. Volponi, H. DePold, R. Ganguli, C. Daguang, *The Use of Kalman Filter and Neural Network Methodologies in Gas Turbine Performance Diagnostics: A Comparative Study*, ASME J. of Eng. for Gas Turbines and Power, vol. 125, 2003.
- [5] T. Kobayashi, D.L. Simon, *A Hybrid Neural Network-Genetic Algorithm Technique for Aircraft Engine Performance Diagnostics*, Paper AIAA-2001-3763, 2001.
- [6] Ph. Kamboukos, K. Mathioudakis, *Multipoint Non-Linear Method for Enhanced Component and Sensor Malfunction Diagnosis*, ASME Paper GT2006-90451, 2006.
- [7] T. Kobayashi, D.L. Simon, *Application of a Bank of Kalman Filters for Aircraft Engine Fault Diagnostics*, ASME Paper GT2003-38550, 2003.
- [8] T. Kobayashi, D.L. Simon, *Evaluation of an Enhanced Bank of Kalman Filters for In-Flight Aircraft Engine Sensor Fault Diagnostics*, ASME Paper GT2004-53640, 2004.
- [9] P. Dewallef, O. Léonard, *Robust Measurement Validation on Jet Engines*, in Proceedings of the fourth European Conference on Turbomachinery, 2001.
- [10] M. Grodent, A. Navez, *Engine Physical Diagnosis using a Robust Parameter Estimation Method*, paper AIAA-2001-3768, 2001.
- [11] P. Dewallef, O. Léonard, *On-Line Performance Monitoring and Engine Diagnostic Using Robust Kalman Filtering Techniques*, ASME Paper GT2003-38379, 2003.
- [12] J.J. Fuchs, *An Inverse Problem Approach to Robust Regression*, 14th IFAC World Congress, 1999.
- [13] S. Borguet, O. Léonard, *A Sensor-Fault-Tolerant Diagnosis Tool Based on a Quadratic Programming Approach*, ASME Paper GT2007-27324, 2007.
- [14] D. Simon, D.L. Simon, *Aircraft Turbofan Engine Health Estimation Using Constrained Kalman Filtering*, ASME Paper GT2003-38584, 2003.
- [15] P. Dewallef, K. Mathioudakis, O. Léonard, *On-Line Aircraft Engine Diagnostics Using a Soft-Constrained Kalman Filter*, ASME Paper GT2004-53539, 2004.
- [16] R. E. Kalman, R. S. Bucy, *New Results in Linear Filtering and Prediction Theory*, Trans. ASME, Series D, Journal of Basic Engineering, vol. 83, 1961.
- [17] P. Dewallef, *Application of the Kalman Filter to Health Monitoring of Gas Turbine Engines : A Sequential Approach to Robust Diagnosis*, PhD. Thesis, University of Liège, 2005.
- [18] S. Haykin, *Kalman Filtering and Neural Networks*, Wiley Series on Adaptive and Learning Systems for Signal Processing, Communication and Control, 2001.
- [19] P.J. Huber, *Robust Statistical Procedures*, Society for Industrial and Applied Mathematics, 1996.
- [20] R. Fletcher, *Practical Methods of Optimization*, Wiley, 2000.
- [21] P. Dewallef, *An Algorithm for Aircraft Engine Performance Monitoring and Sensor Fault Diagnosis*, Technical Report, University of Liège, 2006.
- [22] A. Stamatis, K. Mathioudakis, J. Ruiz, B. Curnock, *Real-Time Engine Model Implementation for Adaptive Control and Performance Monitoring of Large Civil Turbofans*, ASME Paper 2001-GT-0362, 2001.
- [23] B. Curnock, *Obidicote Project – Work Package 4: Steady-State Test Cases*, Technical Report DNS62433, Rolls-Royce Plc, 2000.



A revised version of this article is available here.